Dielectrophoresis of Submicrometer Latex Spheres. 1. Experimental Results

Nicolas G. Green and Hywel Morgan*

Bioelectronics Research Centre, Department of Electronics and Electrical Engineering, University of Glasgow, Rankine Building, Oakfield Avenue, Glasgow G12 8LT, Scotland, UK

Received: July 13, 1998; In Final Form: September 2, 1998

A nonuniform electric field exerts a force on a polarizable particle through the Coulomb interaction with the electric dipole induced in the particle, resulting in a motion termed dielectrophoresis. The magnitude of the force depends on the dielectric properties of both the particle and the medium it is suspended in. As a result, measurement of the dielectrophoretic force provides information about the internal and surface dielectric properties of the particle. This paper presents the first detailed measurements of the dielectrophoretic response of submicrometer particles as a function of electrolyte composition and conductivity, applied field frequency, and particle size. Comparisons are made between the experimental results and the classical theory of the dielectrophoretic force derived from Maxwell−Wagner interfacial polarization. For particles of 557 nm diameter, good agreement is obtained between the experimental results and theory of interfacial polarization taking into account the effects of surface conductance. However, the results for smaller sizes of particle (93, 216, and 282 nm diameter) demonstrate that the theory does not adequately explain the dielectric or dielectrophoretic behavior of colloidal particles. The existence of a second low-frequency dispersion is also apparent in the data, attributable to the polarization of the double layer. The data were compared with a theoretical plot generated by modeling the dispersion in terms of a single Debye relaxation.

1. Introduction

Dielectrophoresis (DEP) can be used as a means of analyzing the dielectric properties of single particles.[1−3] While much effort has been directed at measuring the properties of particles larger than a few micrometers in diameter, there is little data on colloidal particles. The ability to move and study submicrometer particles by dielectrophoresis is now an established fact,[4−8] despite the effects of Brownian motion on these particles. However, the underlying physical mechanisms that govern the dielectric properties of single particles remain to be explored in detail. Accordingly, we have investigated the dielectrophoretic properties of single submicrometer latex particles over a wide range of applied electric field frequencies and electrolyte compositions and concentrations. In part 1 of this paper, we present detailed experimental results and preliminary examinations of the data in light of the Maxwell−Wagner interfacial polarization mechanism as well as the lower frequency relaxation associated with the electrical double layer.

2. Dielectric Theory of an Interface

A dielectric particle suspended in a dielectric medium polarizes following the application of an electric field. The polarization of the interface between the two dielectrics creates an effective dipole moment in the particle. As is the case for all polarization mechanisms, the interfacial mechanism has an associated relaxation time generally referred to as the Maxwell−Wagner relaxation frequency or β-dispersion. For the particular case of linear, isotropic dielectrics and a spherical particle, the effective dipole moment **m** is given by[9]

$$\mathbf{m} = 4\pi a^3 \epsilon_m f_{CM} \mathbf{E} \tag{1}$$

where a is the radius of the particle, ϵ_m is the permittivity of the medium, and **E** is the electric field. The factor f_{CM} represents the frequency dependence of the effective polarizability of the particle (the Clausius−Mossotti factor), given by

$$f_{CM} = \left(\frac{\tilde{\epsilon}_p - \tilde{\epsilon}_m}{\tilde{\epsilon}_p + 2\tilde{\epsilon}_m} \right) \tag{2}$$

where $\tilde{\epsilon}$ indicates a complex permittivity given by $\tilde{\epsilon} = \epsilon - i(K/\omega)$ where ϵ is the permittivity, K is the conductivity, ω is the frequency of the electric field, and $i = (-1)^{1/2}$. The subscripts m and p refer to the suspending medium and particle, respectively. The magnitude of this complex factor varies with the applied field frequency, and an example of the variation of the real part is shown in Figure 1. In calculating this plot, the following parameters were used: $\epsilon_p = 2.55$, $\epsilon_m = 78.5$, $K_p = 0.01$ S/m and $K_m = 0.001$ S/m. For a single interface system, there is a single relaxation with a relaxation time that depends on the combined dielectric properties of the medium and the particle. This relaxation time is given by

$$\tau_\beta = \frac{\epsilon_p + 2\epsilon_m}{K_p + 2K_m} \tag{3}$$

In a nonuniform electric field, a force is exerted on the dipole moment of the particle giving rise to movement referred to as dielectrophoresis (DEP). If the field is not very nonuniform, the time-averaged dielectrophoretic force $\mathbf{F}_{dep}$ is given by the equation

$$\mathbf{F}_{dep} = \mathrm{Re}((\mathbf{m}\cdot\nabla)\mathbf{E}) \tag{4}$$

For a dielectric sphere with the properties outlined above and in low-frequency ac electric fields ($<10^6$ Hz), the Clausius−Mossotti factor is positive and the force acts to move the particle

10.1021/jp9829849 CCC: $18.00
Published on Web 12/15/1998

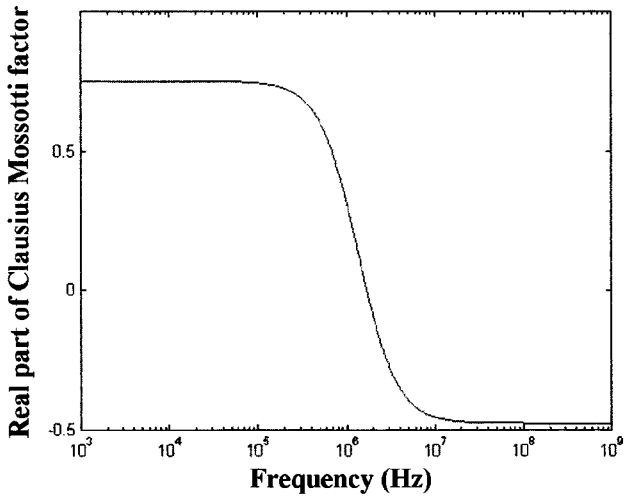

Figure 1. Plot of the variation of the real part of the Clausius−Mossotti factor with applied field frequency for a solid spherical dielectric particle. The relative permittivity of the particle and the suspending medium were 2.55 and 78.5, respectively, and the conductivities were 10^{-2} and 10^{-3} S/m, respectively.

to regions of high field strength. At high frequencies ($>10^6$ Hz), the Clausius−Mossotti factor is negative and the particle moves toward regions of low field strength; see Figure 1. The movement is referred to as positive and negative dielectrophoresis, respectively.

The surface charge density of a particle has been shown to be important in governing its behavior,[5,6,10−12] and the effects on the dielectrophoretic properties of particles are discussed in detail in ref 1. Although latex has a low intrinsic conductivity, dielectric measurements have demonstrated that the measured value of the particle conductivity is high. Researchers in the field attributed the anomaly to the presence of a surface conductance component caused by the movement of counterions to the surface charge on the particle.[12−14] For a sphere with a uniform surface charge density, σ (where the individual charges are of the same sign), and associated counterion mobility μ, O'Konski[14] defined the surface conductance λ as

$$\lambda = \sigma\mu \tag{5}$$

and derived the following expression for the total particle conductivity:

$$K_p = K_{int} + \frac{2\lambda}{a} \tag{6}$$

where K_{int} is the internal particle conductivity and the last term in this expression is the surface conductivity. The presence of this extra component of conductivity increases the Maxwell−Wagner relaxation frequency without introducing an extra dispersion.

Dielectric measurements also indicate that there is a dispersion at frequencies lower than the Maxwell−Wagner,[10,15,16] with its origin also attributed to a surface charge effect. This second polarization mechanism involves changes in the charge density of the electrical double layer generated by the surface potential of the particle.[17,18] The relaxation of this polarization mechanism, called the α-relaxation, occurs at a frequency that is proportional to the particle radius squared.

Accurate measurement of the dielectrophoretic force is difficult to achieve for colloidal particles owing to the effects of Brownian motion[19] and electrically induced fluid flow.[8,20] The presence of the α-relaxation at low frequencies also

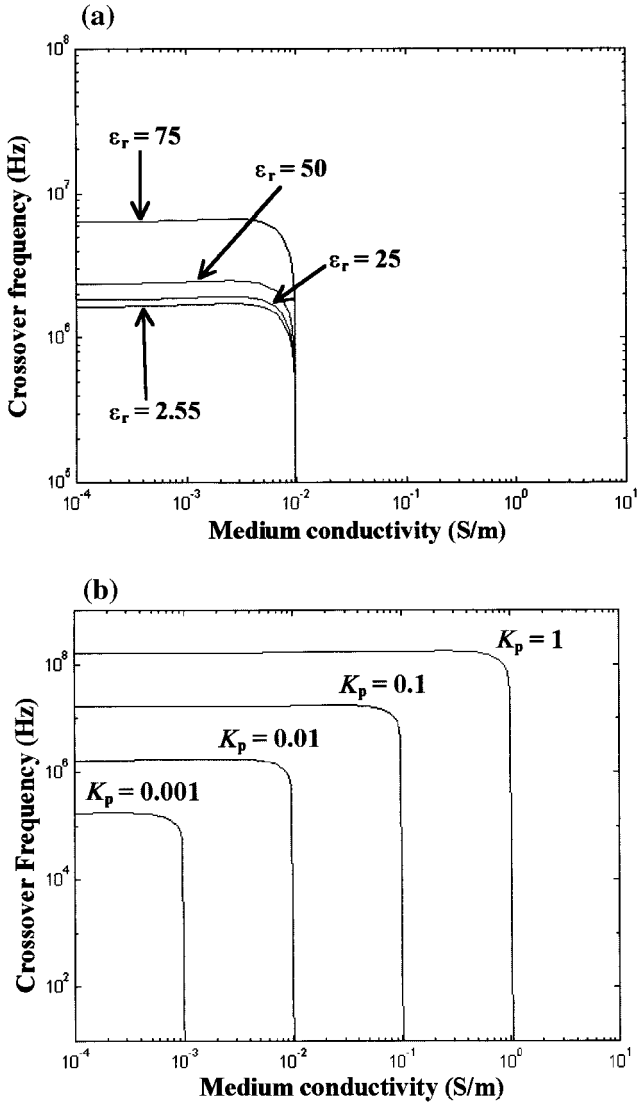

Figure 2. (a) Theoretical plot showing the variation in crossover frequency with medium conductivity as a function of particle relative permittivity, ϵ_r. The conductivity of the particle was 10^{-2} S/m. For a given value of ϵ_r and at low values of K_m, this plot shows that the crossover frequency is constant with increasing conductivity up to a transition value, at which point the crossover frequency falls off rapidly. (b) Theoretical plot showing the variation in crossover frequency with medium conductivity as a function of particle conductivity, K_p. For this plot, the relative permittivity of the particle was 2.55.

complicates simple analysis of the system. Comparatively, the measurement of the frequency at which the dielectrophoretic force is zero or the "crossover point" is simple and can provide information about the internal and surface dielectric properties of the particle. The crossover point is defined to be the frequency at which $\mathrm{Re}((\bar{\epsilon}_p - \bar{\epsilon}_m)/(\bar{\epsilon}_p + 2\bar{\epsilon}_m)) = 0$, where Re indicates the real part.

Figure 2 show plots of the variation of crossover frequency with electrolyte conductivity where the dielectric properties of the particle have been varied as indicated on the figure. The crossover point was numerically calculated from the Clausius−Mossotti factor using a simple binary search algorithm. It can be seen from Figure 2a that varying the particle permittivity (with constant particle conductivity) produces a shift in the crossover frequency across the entire electrolyte conductivity range, but the transition conductivity above which only negative DEP occurs remains unaltered. The effect of changing the

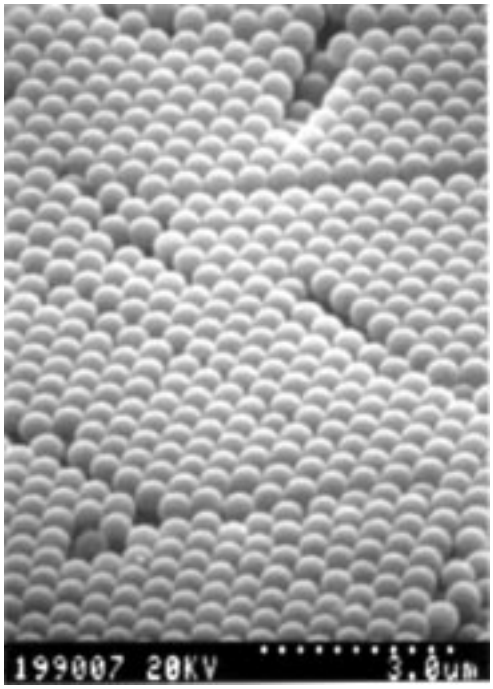

Figure 3. Scanning electron microscope image of 557 nm diameter latex spheres air-dried on a silicon surface. This image shows that the particles are of a uniform size and shape.

particle conductivity, while keeping the permittivity constant, can be seen in Figure 2b.

3. Experimental Section

Electrolytes for the dielectrophoresis experiments were made from three different salts: potassium chloride (KCl), sodium chloride (NaCl), and potassium phosphate buffer, pH 7.2 (KPO_4). The salt used most frequently in the literature for dielectric measurements is potassium chloride (KCl), a symmetrical electrolyte, both in terms of charge (the two ions have equal valency) and in terms of mobility (the potassium ion and the chloride ion have less than a 4% difference in mobility). The other two salts were used in order to determine the effect on the DEP properties of the particles of altering the mobility of either ion in solution. Fluorescent latex spheres (Molecular Probes, Eugene, Oregon) were supplied in a 2 mM azide solution, in sealed containers to prevent contamination. Four sizes of sphere were used in the experiments, with diameters of 557, 282, 216, and 93 nm and were supplied carboxylate-modifed with a high net negative charge at neutral pH. Samples were prepared by diluting the manufacturer's supplied solution either 1:1000 or 1:10000 in each salt solution.

Dielectrophoretic measurements were performed on hyperbolic polynomial electrodes[4−7,21,22] with the center separation varying from 5−50 μm and with a range of applied voltages from 1 to 10 V peak-to-peak provided by analogue or digitally synthesized signal generators.

4. Results

4.1. Size and surface charge measurements. Samples of the spheres were placed on silicon wafers, dried, sputter-coated with metal, and imaged by scanning electron microscopy to determine both if the solutions were contaminated and to check the manufacturer's data on sphere size. Figure 3 shows an SEM of 557 nm diameter spheres forming close-packed structures. The SEM analysis showed that the samples were uncontaminated and that the variation in size of the spheres was within the uncertainty quoted by the manufacturer. The surface charge density of the spheres was determined using a Coulter ζ potential analyzer to measure the particle mobility. This was related to the ζ potential using the Helmholtz−Smoluchowski equation, and the surface charge density was calculated by applying the Gouy−Chapman/Grahame theory of the double layer.[5,18]

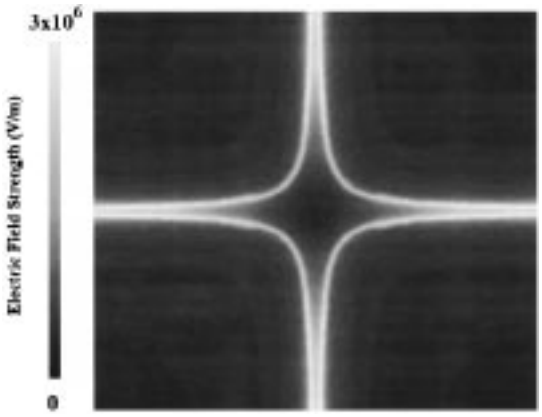

Figure 4. Plot of the electric field magnitude in a plane 100 nm above the surface of a 50 μm diagonal gap polynomial electrode, with an applied potential of 10 V peak-to-peak between adjacent electrodes. The highest field regions (3×10^6 V/m) are found along the electrode edges. In the center of the electrode array, there is a low-field region surrounded by high-field regions that acts as a negative dielectrophoretic potential-energy minimum.

4.2. Electric Field Simulation. Figure 4 shows a plot of the electric field in a plane 100 nm above a set of polynomial electrodes with a separation across the diagonal of 50 μm. The field was solved numerically using commercial finite element software (Maxwell 3-D, Ansoft Corp., Pittsburgh), and as seen in the figure, a maximum in field magnitude lies along the edges of the electrodes. In the center of the four electrodes, there is a minimum in field strength that produces a deep negative-DEP potential energy well.

The DEP force was numerically calculated from this field solution. When particles experience positive DEP, they collect at points of low positive DEP potential energy, corresponding to the high field points along the edges of the electrodes. Under negative DEP, those particles near the middle of the electrode array move into the center, while those away from the middle move away from the electrode edges, either upward or across the electrode surface. At the level of the electrodes, the DEP force is of the same order of magnitude as gravity and the particles will move freely in three dimensions. Electric field and DEP force simulations are discussed in greater detail in the literature.[22,23]

4.3. Dielectrophoretic Behavior. Dielectrophoresis of the latex spheres was observed using a fluorescence microscope (Nikon Microphot) and recorded using a digital camera to video/computer system. Following application of a voltage to the electrodes, the dielectrophoretic movement of the spheres was rapid, with a response and travel time that decreased with decreasing sphere diameter. In all cases, the path of the particles was seen to follow the pattern predicted by the electric field analysis. When particles experienced positive DEP, they collected in lines along the edges of the electrodes, and when the particles experienced negative DEP, they collected at the low-field points in the center of the electrodes or were repelled from the high-field points at the edges of the electrodes. Figure 5 shows four captured video images of 557 nm spheres, suspended in 100 μM KCl, K_m = 1.5 mS/m, on 50 μm polynomial electrodes taken at 3 s intervals. At an applied field frequency

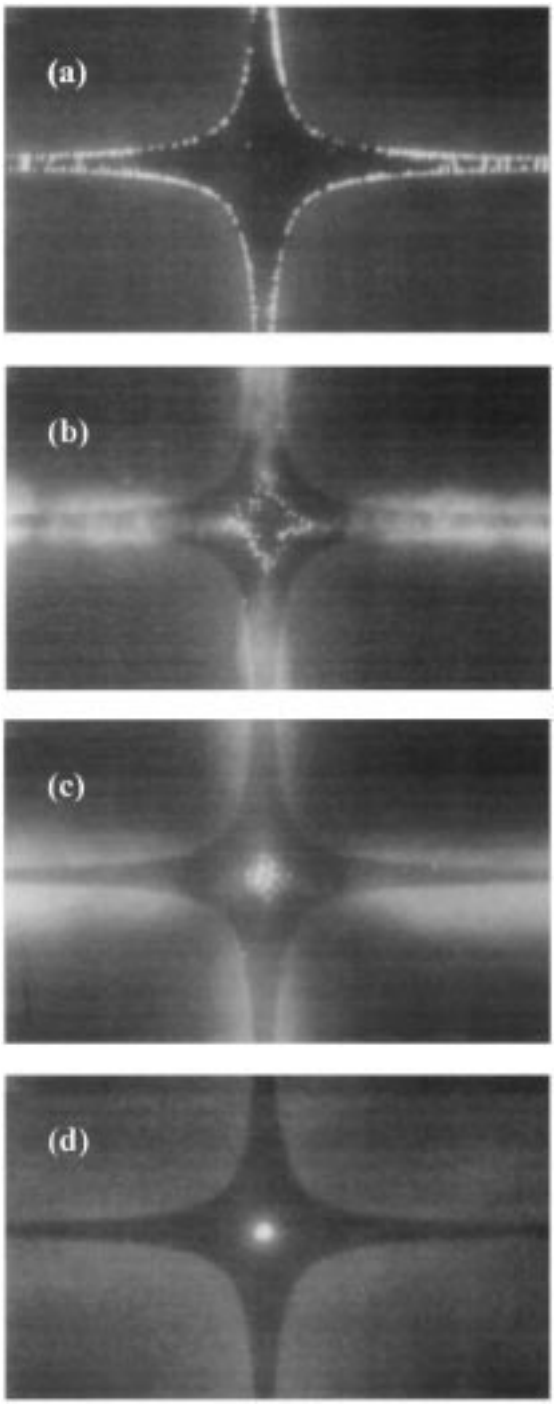

Figure 5. Captured video images of 557 nm diameter latex spheres collecting on 50 μm polynomial electrodes. At 500 kHz and 10 V peak-to-peak, the particles collect at the electrode edges as shown in part a. The sequence b−d is taken at 3 s intervals and shows the result of switching the field frequency to 5 MHz. The particles can be seen to be repelled from the edges under negative dielectrophoretic forces; some particles move upward and some into the center of the electrode array. After 9 s, particles in the center are trapped and held there indefinitely and the remaining particles have diffused back into the suspension, as shown in part d.

of 500 kHz and a potential of 10 V peak-to-peak, the particles were observed to collect at the electrode edges under positive dielectrophoresis as shown in Figure 5a. Figure 5b−d is sequential images showing the result of switching the field to 5 MHz, where the spheres experience negative dielectrophoresis. The spheres close to the center, in the area of the array where the electrodes are noticeably curved, were repelled from the electrode edge into the center of the array. After 9 s, the spheres collected at the center of the array (Figure 5d). Figure 5b−d clearly shows that spheres at the edge of the image, where the electrode edges are almost parallel, moved upward and away from the electrodes rather than into the center. For both cases of positive and negative DEP, the trapped spheres remained in position as long as the electric field was maintained at the same frequency and potential.

As a result of the high electric fields required to produce discernible movement of the particles, heat is dissipated in the electrolyte. In certain circumstances, this gives rise to fluid motion that can affect the particle trajectory.[8,20] Under the experimental conditions used in this work, fluid flow was not significant. When present, detailed observation of the patterns of particle movement could be used to clearly distinguish fluid-driven from DEP-driven particle motion.

4.4. Crossover Measurements. To characterize the dielectric properties of the latex spheres, the crossover frequency of individual particles in a low-volume fraction suspension was measured. This was determined by measuring the range of frequencies over which no dielectrophoretic response of either type was observed. Typically 15−20 particles were analyzed for each conductivity; each point plotted on the figures represents the average of two to six separate measurements using different electrodes. The error in the measurements was less than 1%, and the bars shown in the figures represent the frequency range over which no dielectrophoretic response was observed. The data points without error bars represent the highest frequency at which positive DEP was observed in the case of electrolytes in which no negative DEP was observed. No variation in the mean crossover frequency was observed with voltage, although the frequency range was longer for lower voltages. For conductivities less than 10^{-2} S/m and for high electric fields, fluid flow was observed for frequencies below 10−50 kHz. However, the dielectrophoretic behavior of the particle could be analyzed in the presence of fluid flow, since the flow patterns were distinct and different from particle behavior induced by DEP. This was also the case for higher electrolyte conductivities at frequencies up to 0.5 MHz.

Figure 6a−d shows the variation in crossover frequency with electrolyte conductivity for 557, 282, 216, and 93 nm diameter latex spheres in KCl (pH 6.2−6.6) with conductivities varying from 2.88×10^{-4} to 3.39 S/m. It can be seen from Figure 6a that the crossover frequency from positive to negative DEP remains constant with electrolyte conductivity up to a transition conductivity (which varies with particle diameter) and drops rapidly over a narrow range of conductivities. This is precisely the behavior expected from a particle exhibiting a single Maxwell−Wagner interfacial relaxation (see Figure 2).

Figures 7a−d and 8a−d show the variation in crossover frequencies for the four sizes of sphere for NaCl and KPO_4, respectively. The conductivity of the NaCl solutions (Figure 7) was varied from 2.69×10^{-4} to 1.09 S/m, and the conductivity of the KPO_4, pH 7.2, (Figure 8) was varied from 4.27×10^{-4} to 1.07 S/m. The crossover frequency−conductivity trends are similar to that shown in Figure 6a−d.

5. Discussion

Each of the figures shows that the particle behavior in nonuniform electric fields conforms in some aspects to theoretical expectations. In general, at low frequencies (down to 10 kHz), particles experience positive DEP, while at high frequencies (up to the maximum measured of 20 MHz) they experience negative DEP. This is consistent with previous observations on the DEP properties of submicrometer latex spheres.[5,6] At low

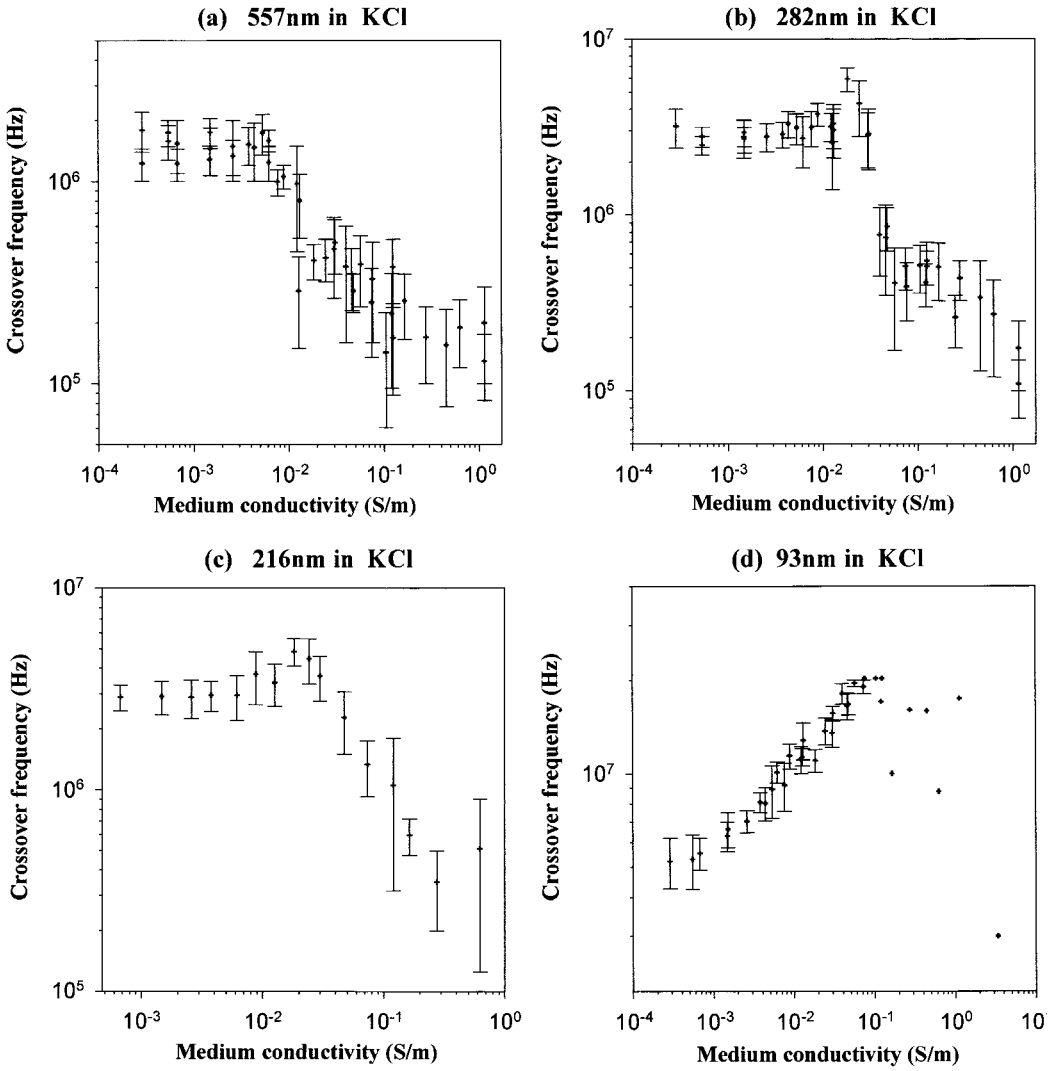

Figure 6. Graph of the experimentally determined crossover frequency as a function of medium conductivity for different sizes of latex spheres in KCl. The vertical bars on each point represent the range of frequencies in which neither positive DEP nor negative DEP was observed. Positive DEP was observed below these points and negative DEP above: (a) 557 nm diameter; (b) 282 nm diameter; (c) 216 nm diameter; (d) 93 nm diameter. In part d, at conductivities below approximately 80 mS/m, positive DEP was observed at low frequencies and negative DEP was observed at high frequencies. The crossover was characterized in this case by a range of frequencies over which both positive and negative DEP was observed, with a mean frequency that increased with medium conductivity. Above 80 mS/m, only positive DEP was observed, and the highest frequency of observation is marked in the figure by a cross without range bars.

electrolyte conductivities and for all of the particles, a crossover frequency in the 1−10 MHz range was observed, which increased with decreasing particle size. As the electrolyte conductivity was increased, the crossover remained relatively constant until, at a value of K_m around 10^{-2} S/m, the crossover frequency dropped to the 100 kHz-1 MHz range.

Interfacial Polarization (*β*-Dispersion) for Large Particles (557 nm Diameter). For all three electrolytes, at low conductivities, the 557 nm spheres exhibit behavior consistent with that expected from Maxwell−Wagner theory (Figure 2). The crossover frequency remains constant at 1.5−1.7 MHz, up to a conductivity of approximately 10^{-2} S/m and then falls at the transition point to a value in the range 1×10^5 to 5×10^5 Hz. The low conductivity behavior can be matched to the Maxwell−Wagner theory to give values for the particle permittivity and conductivity. Figure 9 shows that the closest theoretical fit to the experimental data (at low electrolyte conductivities) for the 557 nm spheres in KCl gives a value of particle conductivity of $K_p = 10 \pm 2$ mS/m. For all the samples, the bulk value of the relative permittivity of latex ($\epsilon_p = 2.55$) was used.[24] In this plot, the limits of the crossover range are represented by crosses and squares.

For NaCl and KPO_4, best fits were obtained with $K_p = 8.4 \pm 0.6$ mS/m and 10 ± 1 mS/m, respectively. The variation in the calculated value is due to the range of frequencies over which the DEP force is too small to produce observable movement. The variation in K_p was greater than our estimate of experimental error and could be reduced by increasing the DEP force (but this increases fluid flow).

The dielectric response of this size of sphere is largely dominated by surface conductance.[5,6,10−18] Since the value of K_p is the same for KPO_4 and KCl, the positive ion must be responsible for the surface conductance. The difference between the response for KCl and NaCl can therefore be attributed to the difference in the mobility of the potassium and sodium ions. Assuming that the internal conductivity of the particles is the same in both salt solutions, then using the bulk values for the mobility of the ions [$\mu_K = 7.69 \times 10^{-8}$ m^2/(V s), $\mu_{Na} = 5.24 \times 10^{-8}$ m^2/(V s)] and adding a scaling factor, A, to eq 6 gives

$$K_p = K_{int} + A\frac{2\sigma\mu}{a} \qquad (7)$$

From this equation, the values of K_{int} and σ can be calculated,

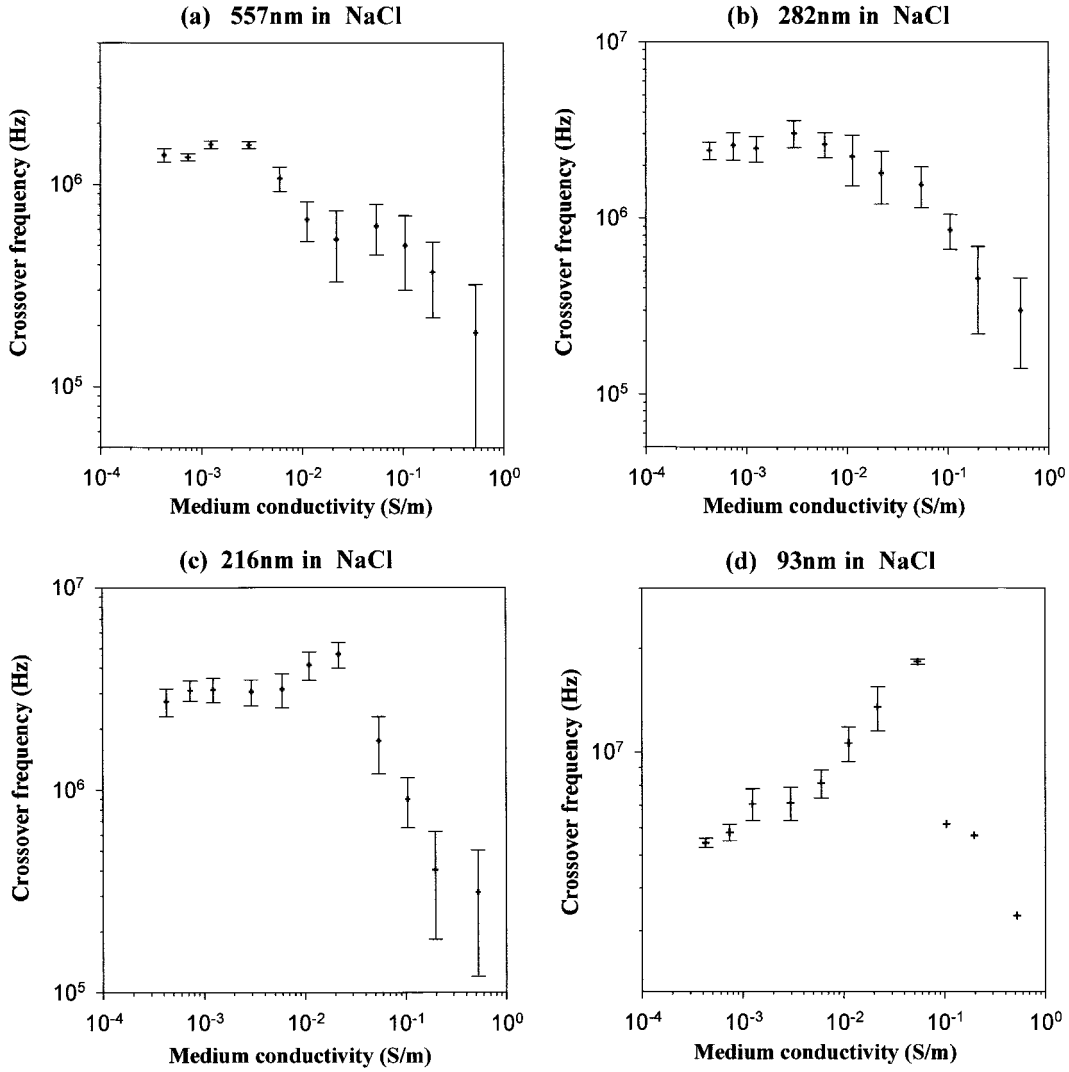

Figure 7. Graph of the experimentally determined crossover frequency as a function of medium conductivity for different diameter latex spheres in NaCl. The bars on either side of the data points represent the range of frequencies in which neither positive DEP nor negative DEP was observed. Positive DEP was observed below these points, and negative DEP was observed above: (a) 557 nm diameter; (b) 282 nm diameter; (c) 216 nm diameter; (d) 93 nm diameter. In part d, in medium conductivities below approximately 70 mS/m, positive DEP was observed at low frequencies and negative DEP at high frequencies. The bars on the first three points represent the range over which both positive and negative DEP was observed, and the bars on the successive five points represent the range over which neither was observed. In medium conductivities above approximately 70 mS/m, only positive DEP was observed with the highest frequency of observation marked by a cross.

using the values of K_p for KCl and NaCl. The results of this calculation give $K_{int} = 5$ mS/m (which is approximately half of the total particle conductivity) and $\sigma = 9$ mC/m^2 (with A set to 1). The measured value for the surface charge density for these particles was $\sigma = 38 \pm 5$ mC/m^2, with the uncertainty arising from a spread in the particle mobility rather than experimental error.[5] Substituting this value of σ in eq 7 with the bulk value of mobility, gives $A = 0.24$. This implies that, in this simple model, either the surface charge density of counterions (i.e., the surface conductance component) is less than that measured for the particle or that the mobility of the counterions close to the surface is approximately a quarter of the bulk value.

Interfacial Polarization for Particles of 93−282 nm Diameter. The results for the 282 and 216 nm diameter latex spheres show slight deviations from the expected behavior; the crossover frequency is constant with electrolyte conductivity up to a certain value, as expected, but then rises slightly before decreasing sharply. This effect is not observed for the 557 nm spheres (although probably present) and dominates the behavior of the 93 nm spheres (Figures 6d, 7d, and 8d). This size of sphere has a crossover frequency that is constant over a narrow range of conductivity, then rises continually with electrolyte conductivity.

For the 282 nm spheres, the five lowest data points can be matched to theory with $K_p = 17 \pm 2.5$ mS/m, for KCl, 15.5 ± 2.5 mS/m, for NaCl, and 17.5 ± 1.5 mS/m, for KPO_4. As an example the best fit for the KCl results is shown in Figure 10. A theoretical curve could be fitted to the data for $K_m < 5$ mS/m to give $K_p = 17$ mS/m. Figure 10 also shows that the theoretical response with $K_p = 35$ mS/m accurately matches the data points for electrolyte conductivities in the range 15−40 mS/m. Over the range 5−15 mS/m, the crossover frequency increases with K_m, a trend that can be seen in the results for the other salts (Figures 7b and 8b). The data for KPO_4 can be satisfactorily fitted to theory in the region of the transition point with $K_p = 37$ mS/m (Figure 8b), but the results for NaCl are obscured by the presence of the α-relaxation (Figure 7b).

The data for the 216 nm spheres can be analyzed in a similar manner to give values for the low K_m regime of $K_p = 17 \pm 3$ mS/m, for KCl, 18.5 ± 2.5 mS/m, for NaCl, and 20 ± 3 mS/m, for KPO_4. The data points around the transition point

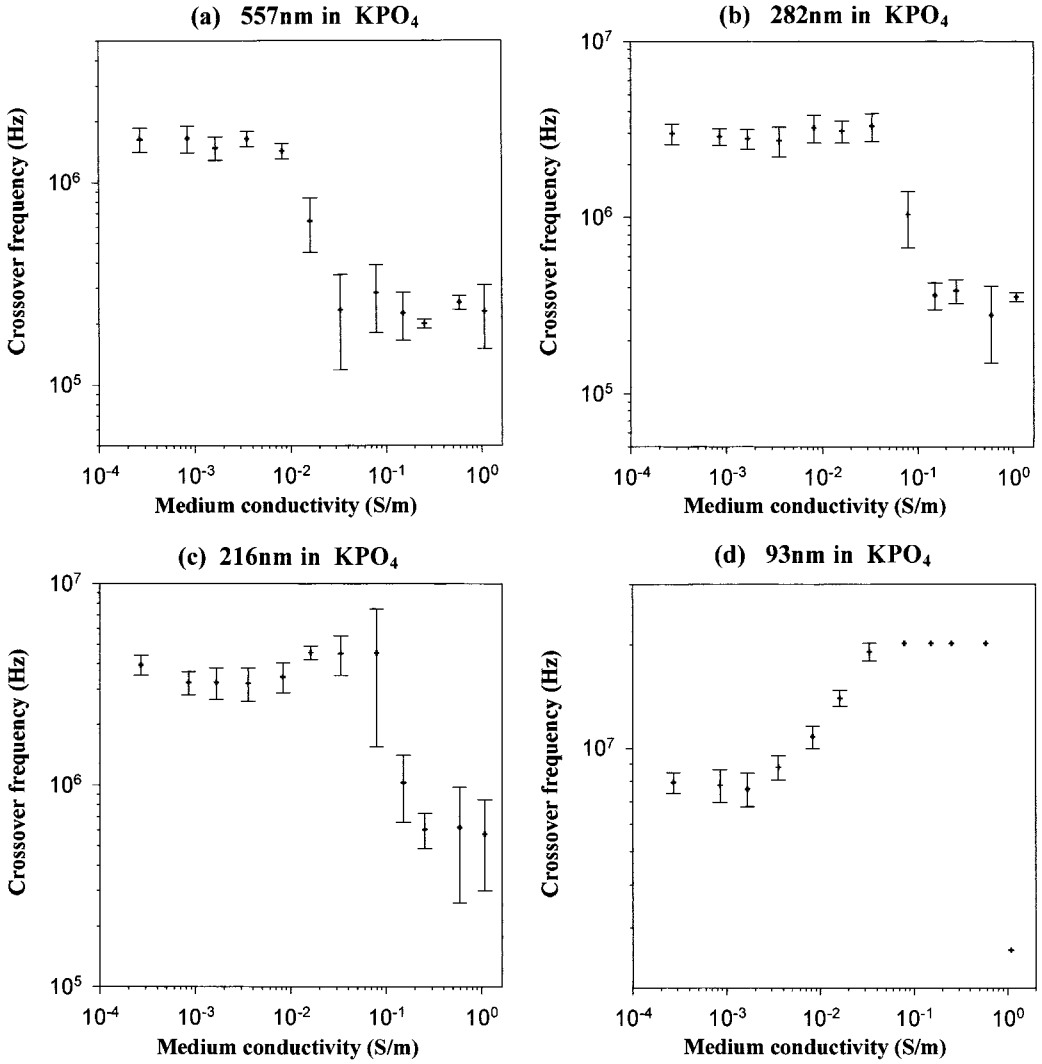

Figure 8. Graph of the experimentally determined crossover frequency as a function of medium conductivity for different diameter latex spheres in KPO_4. Parts a and b show the results for 557 nm and 282 nm diameter spheres. Positive DEP was observed at frequencies below the points and negative DEP above. In the range of frequencies represented by the bars, no DEP was observed for the points below 100 mS/m and both types of DEP were observed for the four points above 100 mS/m. The results for the 216 nm diameter spheres are shown in part c, and in this case, no DEP was observed in the range of frequencies represented by the bars below 200 mS/m and both types of DEP were observed for medium conductivity above 200 mS/m. Again, positive DEP occurred at frequencies above the points and negative DEP below. The results for the 93 nm diameter spheres are shown in part d, where positive DEP was observed below the points and negative DEP was observed at frequencies above the points for medium conductivities below approximately 50 mS/m. In the range of frequencies represented by the bars, both types of DEP were observed and, for medium conductivities above 50 mS/m, only positive DEP was observed, with the maximum frequency of observation represented by a cross.

after the rise in crossover frequency can be matched with $K_p = 45 \pm 5$ mS/m, for KCl, 42 ± 2 mS/m, for NaCl, and 45 ± 5 mS/m, for KPO_4.

There are three possible explanations for the increasing crossover frequency. The first is that, in O'Konski's theory,[14] the surface conductance arises from the counterions present at the interface. In the derivation of the expression given by eq 6, the counterion density is assumed to be equal to the surface charge density of the particle. This is probably true for the case of a particle with a radius substantially greater than the thickness of the double layer (the Debye length, κ^{-1}), i.e., thin double layer with $\kappa a \gg 1$. Where this condition does not hold, the total excess charge in the whole double layer is equal to the surface charge density of the particle and, therefore, the counterion density close to the particle surface is smaller. As a result, in cases where the double layer is not thin, the surface conductance may depend on the Debye length.

The second hypothesis concerns the formation time of the double layer. In cases where O'Konski's theory of surface conductance holds, the frequency of the electric field may be so high that there is insufficient time per cycle for the charge to redistribute and form the double layer.[25] The formation time is given by $\tau = \sigma/\epsilon$, implying that the surface conductance should depend on the electrolyte conductivity, as considered by O'Brien.[26]

The third explanation concerns the electrical potential across the bound component of the double layer, sometimes referred to as the Stern layer. In low-conductivity solutions, where the Debye length is of the order of 10 nm or greater, the drop in potential across the bound layer is quite large. In concentrated salt solutions, the potential drop across the bound layer is low and the potential at the slip plane (outside the bound layer) is relatively high. For the highly charged spheres, there will be a permanent bound layer of charge at the surface and any perturbations to this layer will occur much faster than τ. As a result, the Maxwell−Wagner theory, which considers the polarization of a particle through calculation of the potential

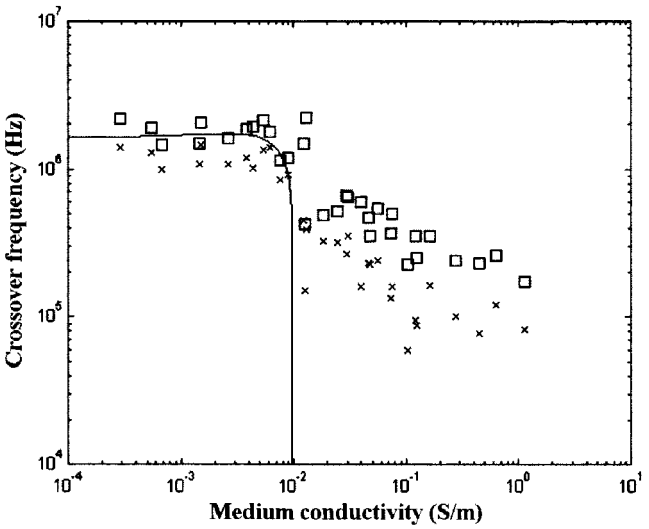

Figure 9. Plot showing the best fit to the experimental data for 557 nm diameter spheres in KCl, from eq 2, with the following parameters for the particle: $K_p = 10$ mS/m, $\epsilon_p = 2.55$, and $\epsilon_m = 78.4$. The symbols represent the plot of the outer limits of the crossover range: (×) point up to which only positive DEP was observed; (□) point above which only negative DEP was observed.

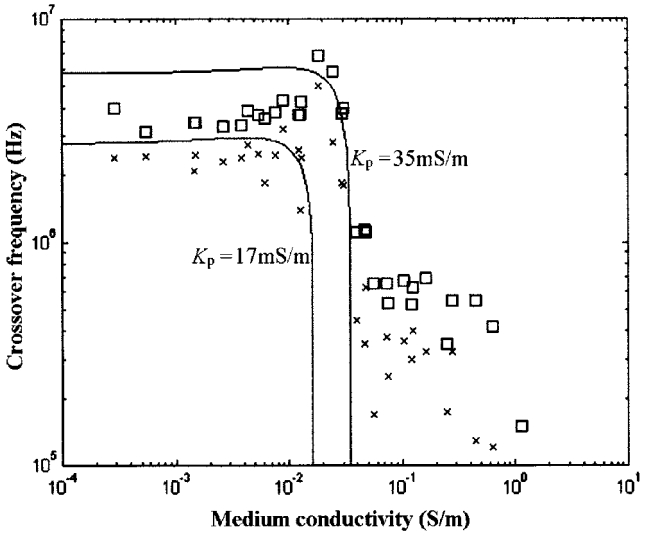

Figure 10. A plot showing the best fit to the experimental data for 282 nm diameter spheres in KCl, from eq 2, with the following parameters for the particle: $\epsilon_p = 2.55$, $\epsilon_m = 78.4$, and $K_p = 17$ mS/m or $K_p = 35$ mS/m. The symbols represent the plot of the outer limits of the crossover range: (×) point up to which only positive DEP was observed; (□) point above which only negative DEP was observed.

at, or electric field across, the interface, should be modified to include this intermediate layer.

The results for the 93 nm diameter spheres show that there is a range of electrolyte conductivities, from 10^{-3} to 10 S/m over which the crossover frequency increases almost a decade for KCl (Figure 6d). For KPO_4 (Figure 8d), it can clearly be seen that there is still a range of conductivities where the crossover frequency, and therefore K_p is constant, occurring at a low value of K_m (Figures 6d, 7d, and 8d). Best fits to the data at low conductivities give $K_p = 32 \pm 6$ mS/m, for KCl, 35 ± 3 mS/m, for NaCl, and 48 ± 4 mS/m, for KPO_4. Figure 11 shows the cross over frequencies for KCl and KPO_4 superimposed on the same two axis plane. This figure indicates that in the conductivity region between 10^{-3} and 2×10^{-1} S/m, where the crossover frequency increases, the data lie along the same line, even though the low K_m data give different values for K_p.

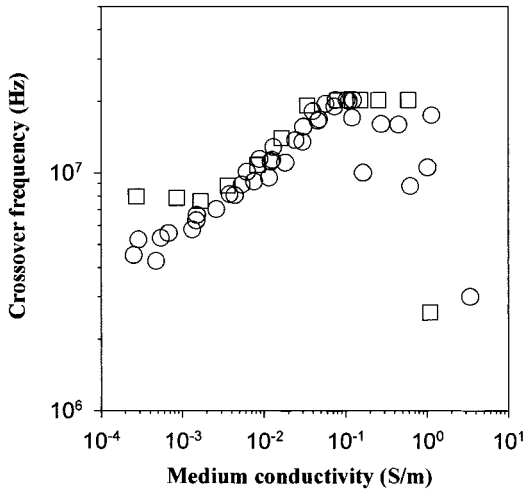

Figure 11. Mean crossover frequency from Figures 6d (□) and 8d (○) superimposed on the same two-axis plane.

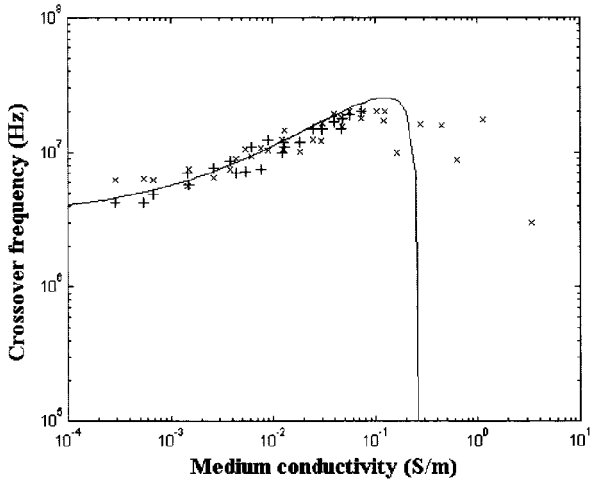

Figure 12. Plot showing the best fit to the experimental data for 93 nm diameter spheres in KCl, from eq 8, with the following parameters for the particle: $\epsilon_p = 2.55$, $\epsilon_m = 78.4$, $K_{int} = 0$, $(2\sigma\mu)/a = 32$ mS/m, $A_1 = 0.2$, and $A_2 = 0.1$.

The increase in K_p with K_m indicated by the data for the smaller particle sizes can be incorporated into the model of Maxwell−Wagner polarization. Modifying eq 6 to include a term proportional to the ratio of the particle radius to the Debye length gives

$$K_p = K_{int} + (A_1 + A_2\kappa a)\frac{2\sigma\mu}{a} \qquad (8)$$

This expression includes an additional component of surface conductance that is inversely proportional to the double layer thickness. Figure 12 shows the theoretical line for the 93 nm spheres calculated using this equation, with $K_{int} = 0$, $(2\sigma\mu)/a = 32$ mS/m, $A_1 = 0.2$, and $A_2 = 0.1$. In this case, a nonzero value for K_{int} cannot be calculated using eq 7, since the ideal interfacial relaxation model does not fit these sizes of particles. The modification to eq 7 successfully accounts for the increase in crossover frequency with K_m, with the slope of the line matching the experimental data. This expression can also be used to fit the data for the larger sizes but with different scaling factors.

Table 1 summarizes the values of K_p for the best fit to the conductivity data where the crossover frequency is constant. The surface charge densities marked as "experimental" were

TABLE 1: Experimental Parameters for the Spheres in Three Different Electrolyte Compositions Obtained Using Eq 6

sphere diameter (nm)	measured σ (mC/m^2) (Coulter counter)	ionic species	K_p (mS/m)	experimental σ (mC/m^2) (crossover data)
557	38 ± 5	KCl	10 ± 2	18.1 ± 20%
		NaCl	8.4 ± 0.6	22.3 ± 7%
		KPO_4	10 ± 1	18.1 ± 10%
282	28 ± 6	KCl	17 ± 2.5	15.6 ± 15%
		NaCl	15.5 ± 2.5	20.8 ± 16%
		KPO_4	17.5 ± 1.5	16.0 ± 8.6%
216	not measured	KCl	17 ± 3	11.9 ± 17.6%
		NaCl	18.5 ± 2.5	19.1 ± 13.5%
		KPO_4	20 ± 3	14.0 ± 15.0%
93	32 ± 8	KCl	32 ± 6	9.7 ± 19%
		NaCl	35 ± 3	15.5 ± 8.6%
		KPO_4	48 ± 4	14.5 ± 8.5%

calculated from K_p using the bulk value for ion mobility and assuming that the particle conductivity arises solely from surface conductance. The values marked as "measured" were determined from the Coulter particle analyzer. The values for K_p indicate that, for the largest size of sphere, the surface conductance arises from movement of the positive ion near the interface as proposed by O'Konski. For the smaller sizes of spheres, less can be inferred about the mechanism involved except that the effect of the negative ion (co-ion) in the electrolyte appears to have an effect for these sizes. This has not been demonstrated in such a clear and concise experiment previously.

Low-Frequency Double Layer Relaxation (α-Relaxation). At high electrolyte conductivity, the crossover data for all particles indicates the presence of a second dispersion at frequencies below the β-relaxation, due to the relaxation of the double layer (the α-relaxation). Using ac impedance methods, this relaxation has been observed for a wide range of particles from cells to latex spheres. The origin of this dispersion is polarization of the double layer charge, either radially or tangential to the particle.[17,18,26−35] Whereas much of the published solution-phase dielectric data can be explained in terms of this model, our data on the dielectrophoretic spectrum of single particles cannot. To a first approximation, an empirical fit to the data can be attempted by adding a second independent Debye relaxation of the form $1/(1 + i\omega\tau_\alpha)$, with the time constant of the relaxation given by $\tau_\alpha = a^2/2D$ or $\tau_\alpha = a^2/2DM$, where D is the ion diffusion constant and M is the electroosmotic contribution to the ion flux of the double layer given by $M = 1 + ((F\sigma)/(RTC_d))$.[6,29,30] The differential capacitance is given by $C_d = \epsilon_m\kappa \cosh((F\zeta)/(2RT))$ where ζ is the ζ potential.[29] Using the bulk values for the ion mobilities and the measured values of ζ potentials, the theoretical crossover frequencies for the 282 and 557 nm spheres in KCl are shown in Figure 13. As can be seen, the fit to the data for the case with the electroosmotic flow is better than that where this component is neglected. However, the predicted response clearly does not match the experimental data and a fuller explanation for the double layer polarization mechanism for a single particle is called for.

6. Conclusion

This paper demonstrates that measurements of the dielectrophoretic behavior of single submicrometer latex particles can be used to uniquely characterize their dielectric properties. By measuring the crossover frequency at which the dielectrophoretic force is zero as a function of medium conductivity, we have shown that the dielectric spectrum of a latex particle has two characteristic dispersions. These are related to the well-known β-dispersion, due to interfacial polarization mechanisms (Maxwell−Wagner polarization), and the α-relaxation, which has its origins in the polarization of the double layer surrounding the particle. For larger sizes of particles (~557 nm diameter), reasonable agreement is obtained between the experimental data and the classical theory of interfacial polarization including surface conductance. The α-relaxation appears in these data as a crossover at lower frequencies in higher medium conductivities. For the smaller sizes of particles, there is a deviation from the predicted response and the size of the deviation increases with decreasing particle size.

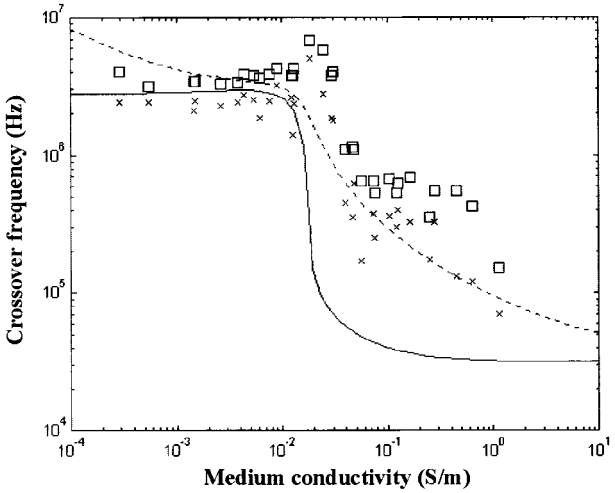

Figure 13. Plot of the mean crossover frequency against medium conductivity for 557 nm diameter spheres in KCl: (×) point up to which only positive DEP was observed; (□) point above which only negative DEP was observed. Also shown are the theoretical crossover frequencies calculated by adding a second Debye dispersion to account for the α-relaxation seen at higher medium conductivities. Curve a is calculated using a relaxation time for the dispersion given by $\tau_\alpha = a^2/(2D)$, whereas curve b is calculated taking into account the electroosmotic contribution to the ion flux around the particle (see text).

Acknowledgment. The authors thank the Engineering and Physical Sciences Research Council for providing a studentship for N. G. Green. We also wish to acknowledge financial assistance from the UK Biotechnology and Biological Sciences Research Council (Grant 17/T05315).

References and Notes

(1) Pohl, H. A. *Dielectrophoresis*; Cambridge University Press: Cambridge, 1978.
(2) Jones, T. B. *Electromechanics of particles*; Cambridge University Press: New York, 1995.
(3) Kaler K. V. I. S.; Jones, T. B. *Biophys. J.* **1990**, *57*, 173.
(4) Green, N. G.; Milner, J. J.; Morgan, H. *J. Biochem. Biophys. Methods* **1997**, *35*, 89.
(5) Green, N. G.; Morgan, H. *J. Phys. D: Appl. Phys.* **1997**, *30*, L41.
(6) Green, N. G.; Morgan, H. *J. Phys. D: Appl. Phys.* **1997**, *30*, 2626.
(7) Hughes, M. P.; Morgan, H.; Rixon, F.; Burt, J. P. H.; Pethig, R. *Biochim. Biophys. Acta* **1998**, *1425*, 119.
(8) Muller, T.; Gerardino, A.; Schnelle, T.; Shirley, S. G.; Bordoni, F.; De Gasperis, G.; Leoni, R.; Fuhr, G. *J. Phys. D: Appl. Phys.* **1996**, *29*, 340.
(9) Stratton, J. A. *Electromagnetic Theory*; McGraw-Hill: New York, 1941.
(10) Schwan, H. P.; Schwarz, G.; Macjuk, J.; Pauly, H. *J. Phys. Chem.* **1962**, *66*, 2626.
(11) Arnold, W. M.; Schwan, H. P.; Zimmerman, U. *J. Phys. Chem.* **1987**, *91*, 5093.
(12) Fricke, H.; Curtis, H. J. *J. Phys. Chem.* **1937**, *41*, 729.
(13) Miles, J. B.; Robertson, H. P. *Phys. Rev.* **1932**, *40*, 583.

(14) O'Konski, C. T. *J. Phys. Chem.* **1960**, *64*, 605.
(15) Schwan, H. P. *Ann. Biomed. Eng.* **1992**, *20*, 269.
(16) Sasaki, S.; Ishikawa, A.; Hanai, T. *Biophys. Chem.* **1981**, *14*, 45.
(17) Schwarz, G. *J. Phys. Chem.* **1962**, *66*, 2636.
(18) Duhkin, S. S. *Dielectric phenomena and the double layer in disperse systems and polyelectrolytes*; John Wiley and Sons: New York, 1974.
(19) Morgan, H.; Green, N. G. *J. Electrostatics* **1997**, *42*, 279.
(20) Ramos, A.; Morgan, H.; Green, N. G.; Castellanos, A. *J. Phys. D: Appl. Phys.* **1998**, *31*, 2338.
(21) Huang, Y.; Pethig, R. *Meas. Sci. Technol.* **1991**, *2*, 1142.
(22) Wang, X.-B.; Huang, Y.; Burt, J. P. H.; Markx, G. H.; Pethig, R. *J. Phys. D: Appl. Phys.* **1993**, *26*, 1278.
(23) Schnelle, T.; Hagedorn, R.; Fuhr, G.; Fiedler, S.; Muller, T. *Biochim. Biophys Acta* **1993**, *1157*, 127.
(24) Lide, D. R., Ed. *CRC Handbook of Chemistry and Physics*, 74th ed.; CRC Press: Boca Raton, 1993−1994.
(25) Bockris, J. O'M.; Reddy A. K. N. *Modern Electrochemistry*; Plenum Press: New York, 1970.
(26) O'Brien, R. W. *J. Colloid Interface Sci.* **1986**, *113*, 81.
(27) Schurr, J. M. *J. Phys. Chem.* **1964**, *68*, 2407.
(28) Fixman, M. *J. Chem. Phys.* **1983**, *78*, 1483.
(29) Lyklema, J.; Duhkin, S. S.; Shilov, V. N. *J. Electroanal. Chem.* **1983**, *143*, 1.
(30) Springer, M. M.; Korteweg, A.; Lyklema, J. *J. Electroanal. Chem.* **1983**, *153*, 55.
(31) Hinch, E. J.; Sherwood, J.; Chen, W. C.; Sen, P. N. *J. Chem. Soc., Faraday Trans.* **1984**, *80*, 535.
(32) Lyklema, J.; Springer, M. M.; Shilov, V. N.; Duhkin, S. S. *J. Electroanal. Chem.* **1986,** *198*, 19.
(33) Lyklema, J. *Fundamentals of Interface and Colloid Science*; Academic Press: London, 1991.
(34) Rosen, L. A.; Saville, D. A. *Langmuir* **1991**, *7*, 36.
(35) van der Wal, A.; Minor, M.; Norde, W.; Zehnder, A. J. B.; Lyklema, J. *J. Colloid Interface Sci.* **1997**, *186*, 71.